MATERIALS CHEMISTRY FRONTIERS

RESEARCH ARTICLE

View Article Online
View Journal | View Issue

Check for updates

Cite this: *Mater. Chem. Front.*, 2022, **6**, 593

Reaction induced supramolecular gelation with the evolution of circularly polarized luminescence†

Kun Li,[ab] Shuyu Chen,[a] Xuefeng Zhu,*[a] Huahua Fan,[ab] Li Zhang *[a] and Minghua Liu *[ab]

Chemical reaction-guided supramolecular gelation has been attracting attention due to its dynamic response and adaptability. We demonstrated here that the direct reduction of the C=N bond to a C–N bond by $NaBH_4$ caused sol-to-gel and gel-to-gel transitions of amphiphilic Schiff bases. 1-Hydroxy-1-naphthaldehyde or 2-hydroxy-1-naphthaldehyde was reacted with an amine-terminated dialkyl glutamide amphiphile (LG) to afford Schiff base 1-NLG or 2-NLG, respectively. These amphiphilic Schiff bases couldn't self-assemble into supramolecular gels in ethanol, while the introduction of $NaBH_4$ led to the formation of a supramolecular gel constituted by 2-NLG *via* reducing the imine to a secondary amine group. It was worth noting that 2-NLG was non-fluorescent due to the occurrence of excited-state intramolecular proton transfer (ESIPT). Interestingly, as the reduction reaction proceeded, the emission of 2-NLG was enhanced and it emitted green fluorescence, and then the green fluorescence emitted by the 2-NLG gel gradually turned into a blue emission. In contrast, only an enhanced blue emission was observed in the case of the 1-NLG assembly upon reduction, instead of sol-to-gel transitions. Accompanied by the formation of a supramolecular gel, the circularly polarized luminescence (CPL) of 2-NLG was also observed, whose colour evolved from green to blue. Furthermore, when 8-hydroxy-1,3,6-pyrenetrisulfonate (HPTS) was doped into the 2-NLG system, both an enhanced emission and an amplified CPL signal of HPTS were found upon the formation of the supramolecular co-gel. This work provided an attractive strategy for fabricating dynamic adaptable soft materials with amplified CPL signals.

Received 25th December 2021,
Accepted 6th January 2022

DOI: 10.1039/d1qm01654g

rsc.li/frontiers-materials

Published on 09 2022. Downloaded on 15/07/24 17:18:53.

Introduction

Supramolecular gels are obtained by the assembly of low molecular weight-gelators (LMWGs) through various non-covalent interactions, including hydrogen bonding, hydrophobic interactions, electrostatic interactions, host–guest interactions, π–π stacking, coordination interactions, *etc.*[1,2] The entangled three-dimensional networks assembled by LMWGs can immobilize solvents to form gels. As a typical soft material, supramolecular gels show smart response to external stimuli,[3–5] such as temperature, light, pH values and chemical reactions, leading to their wide application in the fields of biomedicine, flexible electronic equipment, water purification, sensing and recognition.[6–10]

Considering that the sophisticated functions of organisms rely on highly ordered self-organizing systems and a series of chemical reactions, chemical reaction-guided supramolecular gelation would not only deepen our understanding of the organization of biomolecular systems, but also afford supramolecular materials with intriguing properties, such as adaptation and self-replication.[11–13] Furthermore, the reaction-guided diffusion of gelators would give spatially defined soft matter with concentration gradient or varied chemical compositions at different locations. Chemical reaction-guided supramolecular gels are generally classified into two types based on their reaction mechanisms (bond cleavage or bond formation). In this regard, van Esch *et al.* prepared various supramolecular gels based on the dynamic covalent bond of imine.[14–17] Xu *et al.* did excellent work on enzymatic reaction-guided hydrogels, providing a facile approach to obtaining supramolecular assemblies in a cellular environment.[12,18–20] This enzyme-triggered hydrogel showed potential in the field of cancer imaging and therapy. Ikeda *et al.* found that chemical reactions could induce peptide derivatives to generate a sol-to-gel-to-shrunken gel phase transition, which helped in the development of functional soft materials for valuable biological applications.[21–23] Although some chemical

[a] *Beijing National Laboratory for Molecular Science (BNLMS), CAS Key Laboratory of Colloid, Interface and Chemical Thermodynamics, Institute of Chemistry, Chinese Academy of Sciences, Beijing 100190, P. R. China. E-mail: zhuxf06@iccas.ac.cn, zhangli@iccas.ac.cn, liumh@iccas.ac.cn*

[b] *University of Chinese Academy of Sciences, Beijing 100049, P. R. China*

† Electronic supplementary information (ESI) available: CD and CPL spectra and XRD patterns of NLG systems. See DOI: 10.1039/d1qm01654g

Published on 09 2022. Downloaded on 15/07/24 17:18:53.

reaction-guided supramolecular assemblies have been reported, more sophisticated and transient supramolecular gels exhibiting response to chemical input are desired to broaden the scope of dynamic supramolecular systems.

On the other hand, circularly polarized luminescence (CPL), as an important chiroptical phenomenon,[24–30] has been attracting increasing attention owing to its potential in 3D displays, information storage, and encryption.[31–33] It was demonstrated that supramolecular gels could not only amplify the circular polarization of some CPL-active compounds, but also be functionalized as a "chiral matrix" transferring chiral information to achiral fluorophores to endow them with CPL activity. Herein, we synthesized two Schiff bases (1-NLG and 2-NLG) by reacting the amine-terminated dialkyl glutamide amphiphile (LG) with two aromatic aldehydes.[34] These amphiphilic Schiff bases couldn't self-assemble into supramolecular gels in ethanol. When $NaBH_4$ was added into the 2-NLG suspension, the sol-to-gel transition of 2-NLG took place (Fig. 1). It was reported that the C=N double bond could be selectively reduced to a C–N single bond.[35–37] For example, Cui *et al.* used reducibility of $NaBH_4$ to construct new functionalized COFs that are difficult to obtain in other ways.[36] Here $NaBH_4$ was also supposed to reduce the imine of NLG to a secondary amine. It was worth noting that 1-NLG and 2-NLG were non-fluorescent due to the occurrence of excited-state intramolecular proton transfer (ESIPT).[34] Interestingly, as the reduction progressed, the 2-NLG gel showed a green emission that finally turned into a blue emission. Accompanied by the formation of supramolecular gels, the circularly polarized luminescence (CPL) of 2-NLG with green and blue emissions was also observed, respectively. By contrast, the 1-NLG couldn't form a gel under the same treatment, and only the blue emission without CPL was observed.

Results and discussion

Reaction induced gelation

Fig. 1 shows the assembly evolution of 2-NLG and 1-NLG in ethanol upon addition of $NaBH_4$. Both 2-NLG and 1-NLG couldn't form stable organogels in ethanol and existed as yellow suspensions. Meanwhile, no obvious emission was observed for 2-NLG and 1-NLG in ethanol, which was attributed to ESIPT.[33] Upon addition of two moles of $NaBH_4$, a sol-to-gel transition took place with time in the 2-NLG system, as shown in Fig. 1.

After 4 h, the yellow suspension of 2-NLG turned to yellow gels with green fluorescence emission. After 8 h, the yellow gels of 2-NLG faded to white gels. Meanwhile, the green emission of the 2-NLG gels changed to blue emission. Rheological measurements proved that 2-NLG interacting with $NaBH_4$ for 4 h and 8 h in ethanol showed the typical characteristics of a supramolecular gel (Fig. S1, ESI†). But the gels could not be observed when 2-NLG was in the mixed solvents of ethanol/H_2O, ethanol/acetonitrile or ethanol/DMF upon addition of $NaBH_4$ (Fig. S2, ESI†). By contrast, 1-NLG in ethanol existed as a suspension, and only blue emission was observed upon addition of $NaBH_4$. We also monitored the nanostructural evolution of 2-NLG and 1-NLG with time after addition of $NaBH_4$, as shown in Fig. 1A and B. As for 2-NLG, the sheet structure was observed at the beginning, and gradually, nanofiber structures with a width of about 100 nm and extending to dozens of micrometers were obtained after reduction for 4 h. These nanofiber structures entangled together to form three-dimensional networks, which are the typical nanostructures of supramolecular gels. Further extending the reaction time to 8 h, white gels with blue emission appeared, and the nanofiber structures were preserved. As a reference, the SEM images of 1-NLG in ethanol were investigated upon addition of $NaBH_4$. The lamellar structure gradually transformed to amorphous structures in 1-NLG systems.

Reduction reaction monitored by UV and FL spectra

The UV-vis and fluorescence spectra were used to monitor the reduction of imine to a secondary amine in the NLG system, as shown in Fig. 2 and Fig. S3–S4 (ESI†). The dependence of UV-vis spectra of 2-NLG solution in ethanol on time after addition of

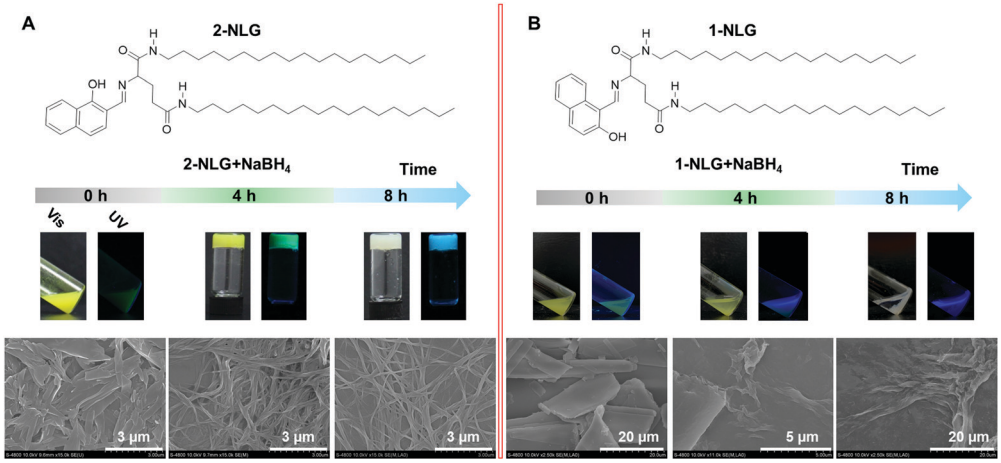

Fig. 1 Evolution of (A) 2-NLG and (B) 1-NLG assemblies in ethanol with the addition of $NaBH_4$; the concentration of 2-NLG and 1-NLG was 1.0×10^{-2} M, and the molar ratio of NLG and $NaBH_4$ was 1 : 2.

 This journal is © The Royal Society of Chemistry and the Chinese Chemical Society 2022

Published on 09 2022. Downloaded on 15/07/24 17:18:53.

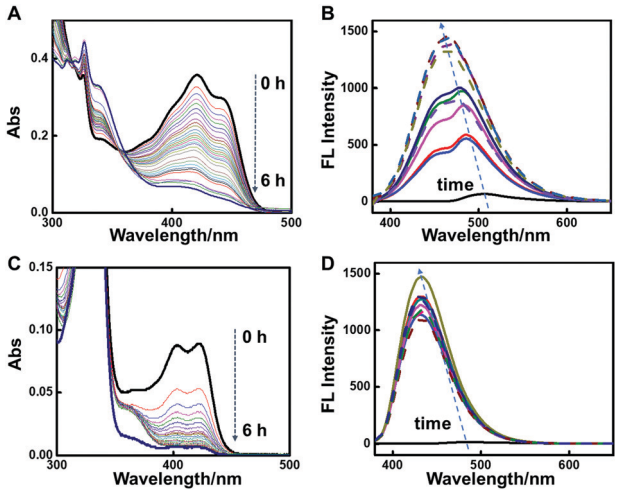

Fig. 2 Variation of UV-vis spectra of 2-NLG solution (A and C) 1-NLG solution as a function of reduction time upon addition of $NaBH_4$ (the concentration of 2-NLG and 1-NLG was 1.2×10^{-4} M, and the molar ratio of NLG and $NaBH_4$ was 1 : 2). Variation of the fluorescence spectra of 2-NLG (B and D) 1-NLG as a function of reduction time upon addition of $NaBH_4$ (the concentration of 2-NLG and 1-NLG was 1.0×10^{-2} M, and the molar ratio of NLG and $NaBH_4$ was 1 : 2).

$NaBH_4$ is shown in Fig. 2A. Two absorption bands at 421 and 445 nm were observed, which were ascribed to the keto-amine form of 2-NLG.[34] After reaction with $NaBH_4$, these bands gradually decreased, indicating that the C=N bond was transformed to the C–N bond. When the concentration of 2-NLG increased to 1.0×10^{-2} M, the absorption bands of 2-NLG showed a red shift relative to its solution state, implying the formation of a 2-NLG assembly, as shown in Fig. S3 (ESI†). The bands in the range of 430–465 nm gradually decreased and disappeared by 8 h (Fig. S3, ESI†), accompanied by the colour change of 2-NLG from yellow to white, implying the breaking of the conjugated system and the disappearance of the keto form. The 2-NLG assembly in ethanol presented a quite weak emission at around 510 nm due to the occurrence of ESIPT.[34] Upon addition of $NaBH_4$, the fluorescence of the 2-NLG system was enhanced, as shown in Fig. 2B. The fluorescence intensity at 486 nm was stronger than that at 432 nm within 6 h. Therefore, the green fluorescence was observed at the beginning. Slowly, the two emission bands merged to form a single band at around 465 nm, which was in accord with the blue emission. This was because the fluorescence of Schiff bases can be enhanced upon reduction due to the inhibition of photoinduced electron transfer (PET) and ESIPT. The UV-vis spectra and fluorescence spectra of 1-NLG upon addition of $NaBH_4$ presented a similar change. The adsorption in the visible range descended progressively and emission at 432 nm was enhanced, as shown in Fig. 2C and D.

CD and CPL spectra studies

1-NLG and 2-NLG contain a chiral carbon atom, and therefore, to investigate the reduction of imine to amine, CD spectroscopy was performed. The CD spectral change of the 2-NLG system was monitored as a function of reaction time, as shown in Fig. 3A. The positive Cotton effects were observed at 435 nm and 460 nm for L-2-NLG, respectively, which was consistent with their absorption band of ketone-form, indicating the chirality transfer from the chiral carbon atom of glutamic acid to the Schiff base chromophore. And the D-2-NLG exhibited negative Cotton effects at 435 and 460 nm, showing a mirror image to that of L-2-NLG, implying the effectiveness of the chirality transfer. The CD signals of 1-NLG at 408 and 432 nm diminished when 1-NLG reacted with $NaBH_4$ for 8 h (Fig. S5, ESI†), indicating that the Schiff base had been reduced. Furthermore, considering that the introduction of $NaBH_4$ caused an emission enhancement and supramolecular gel formation of the 2-NLG system, the CPL spectra of 2-NLG were investigated, as shown in Fig. 3B. The CPL signal was silent at 0 h due to their weak fluorescence emission. When L-2-NLG reacted with $NaBH_4$ for 4 h, L-2-NLG with green emission showed a positive CPL signal around 490 nm, while D-2-NLG gave a negative signal. When L-2-NLG reacted with $NaBH_4$ for 8 h, L-2-NLG transformed into white gels with blue emission, and the CPL signal also showed a slight blue shift to about 465 nm. L-2-NLG exhibited a positive CPL signal, and D-2-NLG showed a negative one. The mirror profiles of the CPL spectrum for the enantiomer of 2-NLG confirmed that the supramolecular gels triggered by $NaBH_4$ reduction exhibited CPL emission. However, no CPL signals were observed in 1-NLG systems, as shown in Fig. S6 (ESI†), although emission enhancement was also observed. Considering that the reduction did not induce gelation of 1-NLG, the circularly polarized luminescence of 1-NLG cannot be amplified enough to be detected by CPL spectroscopy.

IR spectra and XRD patterns

To explore the effect of $NaBH_4$ on the molecular structure and intermolecular interactions of 2-NLG, FTIR spectra were investigated, as shown in Fig. 4A. 2-NLG systems showed vibration bands at 3287 cm^{-1}, 1655 cm^{-1} and 1638 cm^{-1}, which were assigned to the OH stretching vibrations and amide I group,

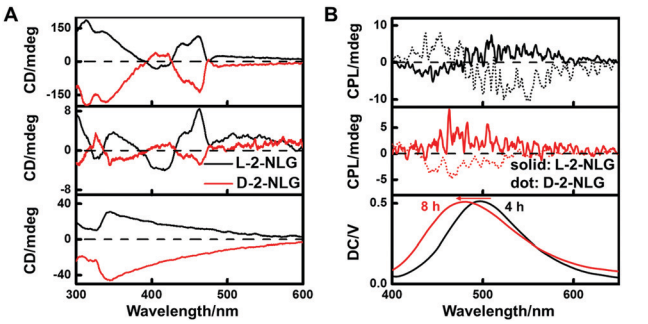

Fig. 3 (A) CD spectra of 2-NLG systems (top: 2-NLG reacted with $NaBH_4$ for 0 h. Middle: 2-NLG reacted with $NaBH_4$ for 4 h. Bottom: 2-NLG reacted with $NaBH_4$ for 8 h). (B) CPL spectra of 2-NLG systems (top: 2-NLG reacted with $NaBH_4$ for 4 h. Middle: 2-NLG reacted with $NaBH_4$ for 8 h. λ_{ex} = 360 nm). The concentration of 2-NLG and 1-NLG was 1.0×10^{-2} M, and the molar ratio of NLG and $NaBH_4$ was 1 : 2.

Published on 09 2022. Downloaded on 15/07/24 17:18:53.

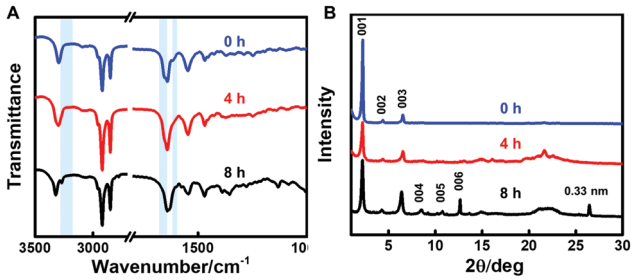

Fig. 4 (A) FTIR spectra and (B) XRD patterns of the 2-NLG system in ethanol (blue: 2-NLG reacted with $NaBH_4$ for 0 h. Red: 2-NLG reacted with $NaBH_4$ for 4 h. Black: 2-NLG reacted with $NaBH_4$ for 8 h).

respectively. In addition, a weak band was observed at 1615 cm^{-1}, ascribed to the C═N vibration. After 2-NLG reacted with $NaBH_4$ for 8 h, the band at 3287 cm^{-1} shifted to 3315 cm^{-1}, suggesting that intramolecular hydrogen bonds (OH—N═C) become weakened. Meanwhile, a new band at 3266 cm^{-1} was observed, which may have resulted from the NH stretching vibrations due to the reduced Schiff bases. The bands in the range of 3000–2800 cm^{-1} assigned to CH stretching vibrations remain unchanged. However, the bands at 1655 cm^{-1} and 1638 cm^{-1} assigned to the amide I band were shifted to 1643 cm^{-1} and 1630 cm^{-1}, respectively, which suggests the enhanced intermolecular hydrogen bonds.[38] Furthermore, the band at 1615 cm^{-1} disappeared, implying that the C═N bond had been reduced. The FTIR spectroscopy results indicated that the C═N bond was reduced to a secondary amine and then enhanced the intermolecular hydrogen bonding between reduced 2-NLG. The reduction of the C═N bond to a secondary amine was also monitored by ^1H NMR (Fig. S7, ESI†). It was found that upon interaction of $NaBH_4$, the proton in CH═N at 8.06 ppm decreased and new peaks at around 3.89 and 3.59 ppm were observed which were ascribed to CH_2–N, as shown in Fig. S7 (ESI†). The variation of the ^1H NMR spectra suggested the reduction of the imine group to a secondary amine. We used integration of the methyl groups in the alkyl chains of 2-NLG as the reference, and the conversion of imine to a secondary amine group was calculated to be about 60% at 4 h and approached 100% at 8 h.

To understand whether the packing modes of nanostructures formed in ethanol changed or not, the XRD patterns of 2-NLG upon treatment with $NaBH_4$ were obtained, as shown in Fig. 4B. From the XRD pattern of 2-NLG systems, well-defined diffractions corresponding to *d*-spacings of 3.87, 2.01, 1.35 and 1.01 nm can be identified. The ratio of the *d*-values follows the proportion of about 1 : 1/2 : 1/3 : 1/4, indicating a lamellar arrangement of 2-NLG systems. According to the Gaussian view, the molecular length of 2-NLG was estimated to be about 3.20 nm,[34] a *d*-spacing of 3.87 nm obtained from the XRD pattern was larger than the length of one molecule of 2-NLG but smaller than the length of two molecules, indicating the formation of a bilayer structure *via* the interdigitation of alkyl chains. After 2-NLG reacted with $NaBH_4$ for 8 h, the lamellar packing of 2-NLG was preserved, and the *d*-spacing was almost kept constant. However, more ordered structure could be obtained, as 005 and 006 diffraction patterns were found. Furthermore, a well-defined diffraction corresponding to the *d*-spacing of 0.33 nm corresponding to π–π* stacking distances was observed,[39] indicating that intermolecular forces were enhanced. In the case of 1-NLG (Fig. S8, ESI†), a bilayer stacking with a large tilt was formed by 1-NLG systems at 0 h due to the ratio of the *d*-values (1 : 1/2 : 1/3 : 1/4). Surprisingly, with the extension of time, the bilayer stacking gradually transformed into the amorphous structure. Therefore, the nanofiber nanostructures cannot be formed by 1-NLG systems due to the weak intermolecular force.

Based on the above analysis, the mechanism of fluorescence enhancement and supramolecular arrangements of 2-NLG systems were proposed and are shown in Fig. 5. Firstly, the intramolecular hydrogen bonding between the C═N and OH groups of 2-NLG disturbed the intermolecular hydrogen bonding of 2-NLG, affecting the self-assembly of 2-NLG. Due to the PET and ESIPT processes, 2-NLG emitted very weak fluorescence. Upon transformation of the C═N bond to the C–N bond, the observed emission was enhanced, which was likely due to the reduction-induced inhibition of the PET and ESIPT processes *via* the reduction of Schiff bases, as shown in Fig. 5. Boron is known to exhibit strong Lewis acidity, which can bond with nucleophilic species and leads to organoboron.[37] In this text, it was suggested that the coordination of boron atoms with N atoms resulted in green emission of the complex. With the extension of reaction time, boron left the reduced 2-NLG, and a remarkable enhancement of fluorescence at 465 nm was observed. The ^1H NMR spectra were used to investigate the coordination of boron atoms with N atoms, as shown in Fig. S7 (ESI†). Upon addition of $NaBH_4$ for about 4 h, a new peak with a chemical shift at 2.35 ppm was observed, implying the existence of BH_3.[40] After 8 h, this peak disappeared, indicating that BH_3 finally left the reduced 2-NLG molecule. With the transformation of C═N to CH_2–N–, intermolecular hydrogen bonds were enhanced and π–π* stacking existed. This may be because a single bond has a higher degree of rotational freedom than

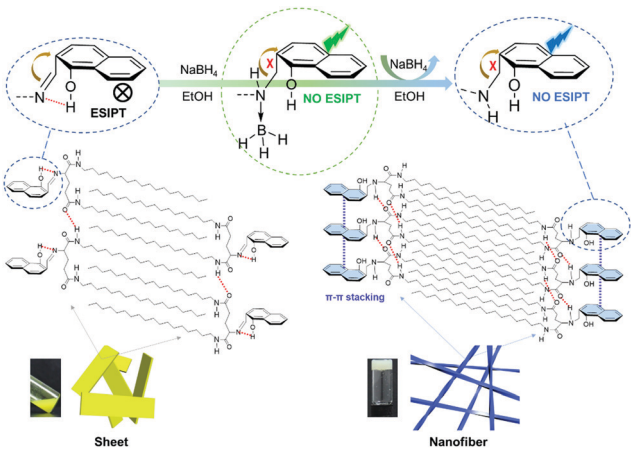

Fig. 5 The illustration of the luminescence enhancement and possible assembly mechanism of 2-NLG upon the addition of $NaBH_4$.

 This journal is © The Royal Society of Chemistry and the Chinese Chemical Society 2022

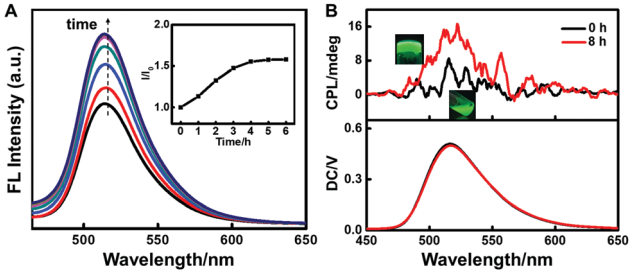

Fig. 6 (A) Emission spectra of 2-NLG systems with HPTS within 6 h (λ_{ex} = 360 nm). Inset: Plot of the changes of emission intensity at 515 nm (I_0: the fluorescence intensity at 0 h; I: the fluorescence intensity at 0–6 h). (B) CPL spectra of 2-NLG systems with HPTS. Inset: Photos under UV light when 2-NLG reacted with $NaBH_4$ for 0 h and 8 h. The concentration of 2-NLG was 1.0×10^{-2} M, and the molar ratio of 2-NLG and HPTS is 10 : 1.

double bonds. The enhanced intermolecular hydrogen bonding and π–π* stacking were attributed to the more ordered packing and formed supramolecular gels with nanofiber structures.

Chirality transfer and enhanced CPL signals

It is reported that supramolecular gels are good medium to transfer or induce the chirality of an achiral dopant in the gels.[41,42] Then, in the following study, we sought the gelation induced chirality transfer to make achiral fluorophores show CPL emission. 8-Hydroxy-1,3,6-pyrenetrisulfonate (HPTS) was chosen due to its conjugate system and strong luminescence.

In the 2-NLG/HPTS mixture, the suspension with green emission was observed, and the fluorescence intensity of HPTS obviously increased with time upon addition of $NaBH_4$. Fig. 6A shows that the emission at 515 nm (λ_{ex} = 360 nm) increased and reached equilibrium within 5 h. Since the emission band of reduced 2-NLG overlapped with the adsorption band of HPTS (Fig. S9, ESI†), the energy transfer from reduced 2-NLG to HPTS may take place and cause the emission enhancement of HPTS. Furthermore, the supramolecular gelation of 2-NLG induced by reduction was supposed to enhance the emission of HPTS due to gel inhibition of non-radiative relaxation channels of HPTS. To understand the gelation induced enhanced emission of HPTS, the fluorescence spectra of HPTS in the 2-NLG system excited at 450 nm was detected, as shown in Fig. S9 (ESI†). The fluorescence intensity of HPTS excited at 450 nm also increased with reduction time, but the increasing degree was lower than that of HPTS/2-NLG excited at 360 nm. Therefore, the enhancement of HPTS with reduction time when excited at 360 nm was derived from the energy transfer from reduced 2-NLG as well as supramolecular gelation. Without 2-NLG, the fluorescence intensity of HPTS decreased slightly with time, and the fluorescence intensity reached a plateau after about 5 hours (Fig. S10, ESI†). It is interesting that the CPL signal of 2-NLG/HPTS after adding $NaBH_4$ at 0 h was very weak. However, when 2-NLG reacted with $NaBH_4$ for 8 h, the supramolecular gels with green emission formed, and a positive CPL signal was detected, as shown in Fig. 6B. This may be because the enhanced π–π* interaction between reduced 2-NLG due to the disappearance of the keto-amine form was conducive to chirality transfer. Therefore, we speculated that the enhancement of intermolecular interactions and the enhancement of gelling ability will enhance the CPL signal.

Conclusions

In summary, we have demonstrated reduction reaction-guided transient supramolecular gel formation. The dynamic self-assembly of two isomeric amphiphilic Schiff bases has been investigated where $NaBH_4$ served as the reduction agent. The sol-to-gel transition of the 2-NLG system took place, and meanwhile, the self-assembled structure of 2-NLG transformed from nanosheets to entangled nanofiber structures, which are the typical structures of supramolecular gels. The reduction of C=N bonds to C–N bonds was proved by UV-vis and FT-IR spectra, resulting in gel formation. Furthermore, upon addition of $NaBH_4$, the fluorescence of 2-NLG was significantly enhanced due to the inhibition of the ESIPT process. With time, the green emission of the gel turned into blue emission and obvious CPL signals with different wavelengths were observed. As for the 1-NLG system, the suspension was kept and only blue emission was observed upon addition of $NaBH_4$, suggesting that a subtle change in the molecular structure could remarkably influence the self-assembly of structures and optical properties. Moreover, when a fluorescent molecule, HPTS, was introduced into the 2-NLG system, CPL signal amplification of HPTS was obtained due to the gel-induced chirality and fluorescence enhancement. This work will promote the design and programmable synthesis of soft materials with adjustable chiroptical activity.

Experimental

Chemical agents

The synthesis and characterization of 2-NLG and 1-NLG have been reported previously by our group.[34] Sodium borohydride was purchased from Guangdong Guanghua Sci-Tech Co., Ltd. Ethanol was obtained from Concord Technology. 8-Hydroxy-1,3,6-pyrenetrisulfonate (HPTS) was obtained from Acros Organics.

Sample preparation

The chemical action of 2-NLG or 1-NLG and $NaBH_4$ was studied in ethanol. First, 1.50 mg of $NaBH_4$ was dissolved in 2.0 mL ethanol by ultrasonication for a few minutes. Then, 1.0 mL $NaBH_4$ solution was put into the sample bottle containing 4.00 mg 2-NLG or 1-NLG, which was sonicated for 5 minutes. The suspension was stored at room temperature, forming an organogel or precipitate (gels and precipitate formed in ethanol at a concentration of 1.0×10^{-2} M for 2-NLG and 1-NLG, and the molar ratio of 2-NLG or 1-NLG and $NaBH_4$ is 1 : 2).

Characterization

Samples at different times (0 h, 4 h, and 8 h) were transferred onto the surface of Si wafers, which were dried in a vacuum

Published on 09 2022. Downloaded on 15/07/24 17:18:53.

Published on 09 2022. Downloaded on 15/07/24 17:18:53.

after 12 h and coated with a layer of Pt particles for scanning electron microscopy (SEM) measurements (Hitachi S-4800 FE-SEM, 10 kV). Infrared characterization was carried out using a Fourier Infrared Spectrometer with an Instrument Model TENSOR-27 from Bruker Spectroscopy. Dried samples on silicon wafers were used for X-ray powder diffraction (XRD) analysis performed on a Rigaku D/Max-2500 X-ray diffractometer with Cu Kα radiation (λ = 1.5406 Å), a voltage of 40 kV, and a current of 200 mA. UV-Vis spectroscopy, fluorescence spectroscopy, circular dichroism (CD), and circularly polarized luminescence (CPL) spectroscopy were performed on Hitachi UV-3900, Hitachi F-4600 fluorescence spectrophotometer, JASCO J-1500 spectrometers, and a JASCO CPL-200 spectrometer, respectively. Quartz cuvettes with a light path of 1 mm or 1 cm were used for meaurement of UV-Vis and fluorescence spectra, respectively. Mechanical properties were studied on a strain-controlled rheometer (Discoevry-DHR-1, TA Instruments) using a cone-plate geometry (20 mm diameter). ^{1}H NMR spectra were recorded on a Bruker Avance 600 spectrometer, in acetonitrile-d_3, and TMS as the internal standard, at 343 K.

Conflicts of interest

There are no conflicts to declare.

Acknowledgements

The authors gratefully acknowledge financial support from the National Natural Science Foundation of China (92156018, 21890734, 21890730, and 21972150) and the CAS Project for Young Scientists in Basic Research (YSBR-027).

Notes and references

1 P. R. A. Chivers and D. K. Smith, Shaping and structuring supramolecular gels, *Nat. Rev. Mater.*, 2019, **4**, 463–478.
2 C. D. Jones and J. W. Steed, Gels with sense: supramolecular materials that respond to heat, light and sound, *Chem. Soc. Rev.*, 2016, **45**, 6546–6596.
3 Y. Pan, Y. Gao, J. Shi, L. Wang and B. Xu, A versatile supramolecular hydrogel of nitrilotriacetic acid (NTA) for binding metal ions and magnetorheological response, *J. Mater. Chem.*, 2011, **21**, 6804–6806.
4 S.-I. Kang, M. Lee and D. Lee, Weak Links to Differentiate Weak Bonds: Size-Selective Response of pi-Conjugated Macrocycle Gels to Ammonium Ions, *J. Am. Chem. Soc.*, 2019, **141**, 5980–5986.
5 W. Tanaka, H. Shigemitsu, T. Fujisaku, R. Kubota, S. Minami, K. Urayama and I. Hamachi, Post-assembly Fabrication of a Functional Multicomponent Supramolecular Hydrogel Based on a Self-Sorting Double Network, *J. Am. Chem. Soc.*, 2019, **141**, 4997–5004.
6 A. M. Vibhute, V. Muvvala and K. M. Sureshan, A Sugar-Based Gelator for Marine Oil-Spill Recovery, *Angew. Chem., Int. Ed.*, 2016, **55**, 7782–7785.
7 X. Cao, Q. Ding, Y. Li, A. Gao and X. Chang, Continuous multi-channel sensing of volatile acid and organic amine gases using a fluorescent self-assembly system, *J. Mater. Chem. C*, 2019, **7**, 133–142.
8 J. Chen, Q. Lin, H. Yao, Y. Zhang and T. Wei, Pillar[5]arene-based multifunctional supramolecular hydrogel: multistimuli responsiveness, self-healing, fluorescence sensing, and conductivity, *Mater. Chem. Front.*, 2018, **2**, 999–1003.
9 Z. Wang, Q. Cheng, P. Xing, Z. Cao and A. Hao, Hydrogen bonded co-assembly of aromatic amino acids and bipyridines that serves as a sacrificial template in superstructure formation, *Soft Matter*, 2019, **15**, 6596–6603.
10 J. Hou, B. Wang, Y. Zou, P. Fan, X. Chang, X. Cao, S. Wang and F. Yu, Molecular Fluorescent Probes for Imaging and Evaluation of Hypochlorite Fluctuations during Diagnosis and Therapy of Osteoarthritis in Cells and in a Mouse Model, *ACS Sens.*, 2020, **5**, 1949–1958.
11 S. Yang, G. Schaeffer, E. Mattia, O. Markovitch, K. Liu, A. S. Hussain, J. Ottele, A. Sood and S. Otto, Chemical Fueling Enables Molecular Complexification of Self-Replicators, *Angew. Chem., Int. Ed.*, 2021, **60**, 11344–11349.
12 H. He, W. Tan, J. Guo, M. Yi, A. N. Shy and B. Xu, Enzymatic Noncovalent Synthesis, *Chem. Rev.*, 2020, **120**, 9994–10078.
13 Y. Zhong, J. Zhan, G. Xu, Y. Chen, Q. Qin, X. Liao, S. Ma, Z. Yang and Y. Cai, Enzyme-Instructed Self-Assembly Enabled Monomer-Excimer Transition to Construct Higher Ordered Luminescent Supramolecular Assembly for Activity-based Bioimaging, *Angew. Chem., Int. Ed.*, 2021, **60**, 8121–8129.
14 H. Wang, L. Liu, S. Bai, X. Guo, R. Eelkema, J. H. van Esch and Y. Wang, Transient supramolecular hydrogels formed by catalytic control over molecular self-assembly, *Soft Matter*, 2020, **16**, 9406–9409.
15 Y. Wang, R. M. de Kruijff, M. Lovrak, X. Guo, R. Eelkema and J. H. van Esch, Access to Metastable Gel States Using Seeded Self-Assembly of Low-Molecular-Weight Gelators, *Angew. Chem., Int. Ed.*, 2019, **58**, 3800–3803.
16 Y. Wang, M. Lovrak, Q. Liu, C. Maity, V. A. A. le Sage, X. Guo, R. Eelkema and J. H. van Esch, Hierarchically Compartmentalized Supramolecular Gels through Multilevel Self-Sorting, *J. Am. Chem. Soc.*, 2019, **141**, 2847–2851.
17 Y. Wang, T. K. Piskorz, M. Lovrak, E. Mendes, X. Guo, R. Eelkema and J. H. van Esch, Transient Supramolecular Hydrogels Formed by Aging-Induced Seeded Self-Assembly of Molecular Hydrogelators, *Adv. Sci.*, 2020, **7**, 1902487.
18 J. Shi, D. Yuan, R. Haburcak, Q. Zhang, C. Zhao, X. Zhang and B. Xu, Enzymatic Dissolution of Biocomposite Solids Consisting of Phosphopeptides to Form Supramolecular Hydrogels, *Chem. – Eur. J.*, 2015, **21**, 18047–18051.
19 X. Du, J. Zhou, J. Shi and B. Xu, Supramolecular Hydrogelators and Hydrogels: From Soft Matter to Molecular Biomaterials, *Chem. Rev.*, 2015, **115**, 13165–13307.
20 Y. Gao, Y. Kuang, Z. Guo, Z. Guo, I. J. Krauss and B. Xu, Enzyme-Instructed Molecular Self-assembly Confers Nanofibers and a Supramolecular Hydrogel of Taxol Derivative, *J. Am. Chem. Soc.*, 2009, **131**, 13576–13577.

 This journal is © The Royal Society of Chemistry and the Chinese Chemical Society 2022

Published on 09 2022. Downloaded on 15/07/24 17:18:53.

21 T. Ohtomi, S. L. Higashi, D. Mori, A. Shibata, Y. Kitamura and M. Ikeda, Effect of side chain phenyl group on the self-assembled morphology of dipeptide hydrazides, *Pept. Sci.*, 2021, **113**, e24200.
22 R. Oosumi, M. Ikeda, A. Ito, M. Izumi and R. Ochi, Structural diversification of bola-amphiphilic glycolipid-type supramolecular hydrogelators exhibiting colour changes along with the gel-sol transition, *Soft Matter*, 2020, **16**, 7274–7278.
23 T. Sugiura, T. Kanada, D. Mori, H. Sakai, A. Shibata, Y. Kitamura and M. Ikeda, Chemical stimulus-responsive supramolecular hydrogel formation and shrinkage of a hydrazone-containing short peptide derivative, *Soft Matter*, 2020, **16**, 899–906.
24 Y. Tan, Y. Okayasu, S. Katao, Y. Nishikawa, F. Asanoma, M. Yamada, J. Yuasa and T. Kawai, Visible Circularly Polarized Luminescence of Octanuclear Circular Eu(III) Helicate, *J. Am. Chem. Soc.*, 2020, **142**, 17653–17661.
25 S. Tsunega, R. Jin, T. Nakashima and T. Kawai, Transfer of Chiral Information from Silica Hosts to Achiral Luminescent Guests: a Simple Approach to Accessing Circularly Polarized Luminescent Systems, *ChemPlusChem*, 2020, **85**, 619–626.
26 K. Liu, Y. Shen, X. Li, Y. Zhang, Y. Quan and Y. Cheng, Strong CPL of achiral liquid crystal fluorescent polymer-viathe regulation of AIE-active chiral dopant, *Chem. Commun.*, 2020, **56**, 12829–12832.
27 M. Hu, H. Feng, Y. Yuan, Y. Zheng and B. Tang, Chiral AIEgens – Chiral recognition, CPL materials and other chiral applications, *Coord. Chem. Rev.*, 2020, **416**, 213329.
28 Y. Yuan, M. Hu, K. Zhang, T. Zhou, S. Wang, M. Liu and Y. Zheng, The largest CPL enhancement by further assembly of self-assembled superhelices based on the helical TPE macrocycle, *Mater. Horiz.*, 2020, **7**, 3209–3216.
29 H. Wang, L. Xu and M. Liu, Supramolecular Gel Based on Amphiphilic Quinoxaline: Chirality Inversion and Chiroptical Switch with Multiple Stimuli-Responsiveness, *Acta Phys.-Chim. Sin.*, 2020, **36**, 1910036.
30 Y. Sang, J. Han, T. Zhao, P. Duan and M. Liu, Circularly Polarized Luminescence in Nanoassemblies: Generation, Amplification, and Application, *Adv. Mater.*, 2020, **32**, 1900110.
31 J. Liang, A. Hao and P. Xing, Noncovalently Modulated Chiral Nanoclays for Circularly Polarized Luminescence Color Conversion, *ACS Appl. Mater. Interfaces*, 2020, **12**, 45665–45672.
32 Y. Chen, P. Lu, Z. Li, Y. Yuan, Q. Ye and H. Zhang, Dual Stimuli-Responsive High-Efficiency Circularly Polarized Luminescence from Light-Emitting Chiral Nematic Liquid Crystals, *ACS Appl. Mater. Interfaces*, 2020, **12**, 56604–56614.
33 L. Zhang, H. Wang, S. Li and M. Liu, Supramolecular chiroptical switches, *Chem. Soc. Rev.*, 2020, **49**, 9095–9120.
34 Q. Jin, S. Chen, H. Jiang, Y. Wang, L. Zhang and M. Liu, Self-Assembly of Amphiphilic Schiff Base and Selectively Turn on Circularly Polarized Luminescence by Al^{3+}, *Langmuir*, 2018, **34**, 14402–14409.
35 P. J. Waller, S. J. Lyle, T. M. O. Popp, C. S. Diercks, J. A. Reimer and O. M. Yaghi, Chemical Conversion of Linkages in Covalent Organic Frameworks, *J. Am. Chem. Soc.*, 2016, **138**, 15519–15522.
36 C. Yuan, S. Fu, K. Yang, B. Hou, Y. Liu, J. Jiang and Y. Cui, Crystalline C–C and C═C Bond-Linked Chiral Covalent Organic Frameworks, *J. Am. Chem. Soc.*, 2021, **143**, 369–381.
37 Z. Ma, Z. Wang, X. Meng, Z. Ma, Z. Xu, Y. Ma and X. Jia, A Mechanochromic Single Crystal: Turning Two Color Changes into a Tricolored Switch, *Angew. Chem., Int. Ed.*, 2016, **55**, 519–522.
38 G. Ouyang, L. Ji, Y. Jiang, F. Wuerthner and M. Liu, Self-assembled Mobius strips with controlled helicity, *Nat. Commun.*, 2020, **11**, 5910.
39 Y. Wang, K. Wan, F. Pan, X. Zhu, Y. Jiang, H. Wang, Y. Chen, X. Shi and M. Liu, Bamboo-like pi-Nanotubes with Tunable Helicity and Circularly Polarized Luminescence, *Angew. Chem., Int. Ed.*, 2021, **60**, 16615.
40 C. Jaska, K. Temple, A. Lough and I. Manners, Transition metal-catalyzed formation of boron–nitrogen bonds: Catalytic dehydrocoupling of amine–borane adducts to form aminoboranes and borazines, *J. Am. Chem. Soc.*, 2003, **125**, 9424–9434.
41 S. Du, X. Zhu, L. Zhang and M. Liu, Switchable Circularly Polarized Luminescence in Supramolecular Gels through Photomodulated FRET, *ACS Appl. Mater. Interfaces*, 2021, **13**, 15501–15508.
42 H. Fan, H. Jiang, X. Zhu, Z. Guo, L. Zhang and M. Liu, Switchable circularly polarized luminescence from a photoacid co-assembled organic nanotube, *Nanoscale*, 2019, **11**, 10504–10510.